ApoA-I cleaved by transthyretin has reduced ability to promote cholesterol efflux and increased amyloidogenicity

Márcia Almeida Liz,[*,†] Cláudio M. Gomes,[§] Maria João Saraiva,[*,†] and Mónica Mendes Sousa[1,*]

Molecular Neurobiology Group,* Instituto de Biologia Molecular e Celular (IBMC), Porto, Portugal; Instituto de Ciências Biomedicas Abel Salazar (ICBAS),† University of Porto, Porto, Portugal; and Instituto Tecnologia Química e Biológica,§ Universidade Nova de Lisboa, Oeiras, Portugal

Abstract A fraction of plasma transthyretin (TTR) circulates in HDL through binding to apolipoprotein A-I (apoA-I). Moreover, TTR is able to cleave the C terminus of lipid-free apoA-I. In this study, we addressed the relevance of apoA-I cleavage by TTR in lipoprotein metabolism and in the formation of apoA-I amyloid fibrils. We determined that TTR may also cleave lipidated apoA-I, with cleavage being more effective in the lipid-poor preβ-HDL subpopulation. Upon TTR cleavage, discoidal HDL particles displayed a reduced capacity to promote cholesterol efflux from cholesterol-loaded THP-1 macrophages. In similar assays, TTR-containing HDL from mice expressing human TTR in a TTR knockout background had a decreased ability to perform reverse cholesterol transport compared with similar particles from TTR knockout mice, reinforcing the notion that cleavage by TTR reduces the ability of apoA-I to promote cholesterol efflux. As amyloid deposits composed of N-terminal apoA-I fragments are common in the atherosclerotic intima, we assessed the impact of TTR cleavage on apoA-I aggregation and fibrillar growth. We determined that TTR-cleaved apoA-I has a high propensity to form aggregated particles and that it formed fibrils faster than full-length apoA-I, as assessed by electron microscopy. Our results show that apoA-I cleavage by TTR may affect HDL biology and the development of atherosclerosis by reducing cholesterol efflux and increasing the apoA-I amyloidogenic potential.—Liz, M. A., C. M. Gomes, M. J. Saraiva, and M. M. Sousa. **ApoA-I cleaved by transthyretin has reduced ability to promote cholesterol efflux and increased amyloidogenicity. *J. Lipid Res.* 2007.** 48: **2385–2395.**

Supplementary key words high density lipoprotein • reverse cholesterol transport • apolipoprotein A-I • apolipoprotein A-I amyloidosis • atherosclerosis

Transthyretin (TTR), a homotetrameric protein (1), is the plasma carrier for both thyroxine and retinol, in the latter case through binding to retinol binding protein (RBP) (2). We previously determined that TTR has several connections to apolipoprotein A-I (apoA-I) biology: *i*) under physiological conditions, a fraction of plasma TTR circulates in HDL through binding to apoA-I (3); *ii*) similar to chymase (4), TTR is able to cleave the C terminus of apoA-I after phenylalanine 225 (5); and *iii*) under pathological conditions, an amyloidogenic apoA-I mutation was identified in which fibrils presented both mutant apoA-I N-terminal fragments and wild-type TTR (6), suggesting that TTR might influence the generation of apoA-I fragments and apoA-I deposition.

The mature form of apoA-I, the major protein component of HDL, can bind lipids to form structures such as *i*) small lipid-poor complexes, *ii*) flattened discoidal particles of various discrete sizes containing only polar lipids (preβ-HDL), and *iii*) polymorphic spherical particles (α-HDL), ranging from small particles containing only one molecule of apoA-I and a few phospholipids to large particles containing up to four molecules of apoA-I in addition to other lipoproteins and a core enriched with cholesteryl esters (CEs). The α-HDLs account for ~90% of all plasma apoA-I. In addition to a structural function, apoA-I is responsible for the major functions of HDL: its central region has been implicated in the activation of LCAT (7), whereas its C-terminal domain, including the region cleaved by TTR, has been shown as especially important for promoting cholesterol efflux from cholesterol-loaded macrophages (4). These functions are pivotal for reverse cholesterol transport, in which peripheral cell cholesterol is returned to the liver for subsequent metabolism. In this process, nascent discoidal HDL, the preβ particles, interact with peripheral cells, including macrophages, to promote the removal of excess free cholesterol.

The pathways through which HDL contributes to cholesterol efflux may occur through two mechanisms: *i*) a relatively nonspecific interaction of apoA-I present in α-HDL with cell membranes, facilitated by the scavenger receptor class B type I (SR-BI), followed by passive diffusion of free cholesterol; and *ii*) a high-affinity interaction of lipid-free and lipid-poor apoA-I (preβ-HDL) with the mem-

Manuscript received 30 March 2007 and in revised form 25 July 2007.

Published, JLR Papers in Press, August 10, 2007.
DOI 10.1194/jlr.M700158-JLR200

[1] To whom correspondence should be addressed.
e-mail: msousa@ibmc.up.pt

brane transporter ABCA1 (8). After cholesterol uptake, discoidal preβ-HDLs are converted into CE-enriched spherical α-HDLs as a result of the action of the plasma cholesterol-esterifying enzyme LCAT (9). CEs in mature α-HDL may then be removed by several different pathways, including selective uptake by the liver, mediated by SR-BI, the high-affinity HDL receptor that recognizes apoA-I and other apolipoproteins and is expressed in the liver and steroidogenic tissues (10). The process of reverse cholesterol transport is especially critical for macrophages, which lack the ability to regulate the influx of cholesterol from modified LDL and therefore are easily transformed into cholesterol-loaded foam cells (11), typical of early atherosclerotic lesions (9).

In preβ-HDL, the C-terminal portion of apoA-I has been shown to be remarkably sensitive to proteolysis (12), which is probably related to the lack of an organized secondary structure of this region. In fact, several proteases found in the arterial intima, such as elastase (13), metalloproteases (14), plasmin and plasma kallikrein (15), and the mast cell proteases chymase and tryptase (8), degrade apoA-I in preβ-HDL particles in vitro. A crucial prerequisite for the action of HDL particles as efficient acceptors of cellular cholesterol is their integrity; in agreement with this concept, apoA-I cleavage by the above proteases has been widely demonstrated to impair the high-affinity component of cellular cholesterol efflux. It is also noteworthy that beyond acting on the balance of CE uptake/efflux by macrophages, apoA-I is further related to atherosclerosis, as N-terminal fragments of apoA-I are frequently found as amyloid deposits in the aortic intima (16).

In the present work, we investigated the relevance of apoA-I cleavage by TTR in HDL biology and in the apoA-I amyloidogenic potential.

METHODS

Mice

Mice were handled according to European Union and national rules, and all of the studies performed were approved by the Portuguese General Veterinarian Board. TTR knockout mice (TTR KO) (17) and human TTR transgenic mice in a TTR KO background (hTTR×TTR KO) (18) in the 129/Sv background were maintained at 24 ± 1°C under a 12 h light/dark cycle and fed regular chow and tap water ad libitum. All animals were accustomed to regular handling.

Production of recombinant human TTR

Recombinant human TTR was produced in *Escherichia coli* D1210 transformed with a pINTR plasmid carrying the wild-type TTR cDNA, as already described (5). Briefly, after osmotic shock, proteins were separated on a diethylaminoethyl cellulose ion-exchange chromatography column (Whatman). Negatively charged protein fractions were dialyzed and lyophilized, and TTR was isolated by preparative electrophoresis on a native Prosieve agarose gel (FMC), according to the supplier's instructions. After electrophoresis, the TTR band was excised from the gel and electroeluted in an Elutrap system (Schleicher and Schuell) in 5 mM Tris and 38 mM glycine, pH 8.3, at 150 V and 4°C overnight.

Lipoprotein preparation

ApoA-I from human plasma was from BioChemika. Spherical high density lipoproteins (sHDLs), enriched in α-HDL and a minor subpopulation of preβ-HDL (d = 1.063–1.210 g/ml), were prepared from freshly isolated normolipidemic human plasma by sequential ultracentrifugation using a KBr/NaCl gradient (19). Mouse sHDLs (d = 1.063–1.210 g/ml) were isolated by ultracentrifugation as described for human plasma. Reconstituted discoidal preβ-migrating high density lipoproteins (rHDLs) were prepared by the sodium cholate dialysis technique (20) using POPC (Avanti Polar Lipids), cholesterol (Sigma), apoA-I, and sodium cholate (Sigma) in a molar ratio of 80:8:1:80, respectively. Lipoprotein concentrations are expressed in terms of their protein content, as determined by the method of Lowry et al. (21). TTR concentration in HDL was determined by the Laurel method (22).

ApoA-I cleavage by TTR

Lipid-free apoA-I, rHDL, or sHDL particles were incubated with TTR in an equimolar ratio in 50 mM Tris, pH 7, overnight at 37°C. Control incubations were performed in the absence of TTR. For lipid-free apoA-I and rHDL particles, after incubation, reactions were analyzed on 15% SDS-PAGE gels and visualized by Coomassie Blue staining to determine the extent of apoA-I cleavage by TTR. For sHDL particles, proteins were separated on a 15% SDS-PAGE gel and then transferred to a nitrocellulose membrane (Amersham) for immunoblot identification of apoA-I and assessment of cleavage by TTR. For Western analysis, membranes were blocked with blocking buffer (10% nonfat dried milk in PBS) and incubated overnight at 4°C with goat polyclonal anti-human apoA-I (Calbiochem; 1:1,000 in blocking buffer) and subsequently for 1 h at room temperature with anti-goat IgG horseradish peroxidase complex (The Binding Site; 1:10,000 in blocking buffer). Immunoblots were developed using 3,3′-diaminobenzidine (Sigma) as the substrate. For analysis of sHDL subpopulations (α-HDL and preβ-HDL) upon TTR treatment, reactions were prepared as described above, concentrated, resuspended in 10 μl of barbital buffer (0.06 M, pH 8.6), electrophoresed at 40 mA for 2 h on 1% agarose gels in barbital buffer, and subsequently stained with Coomassie Blue. Migration patterns were compared with the migration of albumin in 2 μl of a human serum sample. The extent of apoA-I degradation by TTR was determined by densitometry. In every case, at least three independent experiments were performed. Results are presented as averages ± SEM.

TTR detection in sHDL

TTR detection in sHDL subpopulations was performed by Western blot analysis. Briefly, 10 μg of sHDL particles was separated on 1% agarose gels in barbital buffer as described above. Gel regions corresponding to the α-HDL and preβ-HDL subpopulations were identified based on their migration properties compared with similar Coomassie Blue-stained samples loaded in parallel. Unstained gel regions corresponding to the α-HDL and preβ-HDL subpopulations were excised from the agarose gel, applied to a second-dimension 15% SDS-PAGE gel, and then transferred to a nitrocellulose membrane. Western analysis was performed as described above using the following primary antibodies: rabbit polyclonal anti-TTR (DAKO; 1:1,000) and rabbit polyclonal anti-RBP (The Binding Site; 1:500). Western analysis using goat polyclonal anti-apoA-I (Calbiochem; 1:1,000) was performed to normalize the amount of loaded α-HDL and preβ-HDL.

Cholesterol efflux assays

For studies using THP-1 cells (European Cell Culture Collection), cells were routinely grown in suspension in RPMI medium

(Invitrogen) containing 10% fetal bovine serum (Invitrogen), 50 U/ml penicillin, and 50 μg/ml streptomycin (THP-1 complete medium). For each experiment, THP-1 monocytes were differentiated into macrophages by plating 400,000 cells/well on 12-well tissue culture plates (Corning) and by supplementing the medium with 50 ng/ml phorbol 12-myristate 13-acetate (Sigma). After the differentiation period (3 days), THP-1-derived macrophages were incubated for 24 h in complete medium containing 0.5 μCi of [^{3}H]cholesterol (Amersham) per well. For studies of apoA-I binding to ABCA1, human embryonic kidney 293 cells overexpressing ABCA1 (HEK293-ABCA1) and control untransfected cells (HEK293) (a kind gift from Dr. Michael R. Hayden, University of British Columbia, Vancouver) were used. For cholesterol efflux assays, cells were plated on 12-well tissue culture plates (40,000 cells/well) in DMEM (Invitrogen) supplemented with 10% fetal bovine serum, 50 U/ml penicillin, and 50 μg/ml streptomycin (HEK293 complete medium). When cultures reached ~50% confluence, cells were incubated for 24 h in complete medium containing 0.5 μCi of [^{3}H]cholesterol. For both THP-1 and HEK293 cells, [^{3}H]cholesterol-loaded cells were washed and subsequently incubated with 25 μg/ml different cholesterol acceptors (as detailed in Results), either intact or cleaved by TTR, in medium containing 0.2% fatty acid-free BSA (FAF-BSA; Sigma), 50 U/ml penicillin, and 50 μg/ml streptomycin. Four hours later, media were collected and cells were lysed with 0.1 M NaOH; the radioactivity associated with the conditioned media and cells was measured in a Microbeta Counter (Perkin-Elmer). When applicable, the amount of total protein in the cell lysate was determined by the Lowry method. The percentage of cholesterol efflux was calculated as [cpm in the medium at 4 h/(cpm in the medium at 4 h + cpm in the cells)] × 100. For each condition, the percentage of cholesterol efflux in the absence of cholesterol acceptor was subtracted. Data are presented as averages ± SD.

For the analysis of ABCA1 expression, total RNA from HEK293-ABCA1 and HEK293 cells was isolated using Trizol (Invitrogen), and cDNA was obtained using the SuperScript II kit (Invitrogen), according to the manufacturer's protocol. Subsequently, PCR was performed using specific primers designed with PRIMER3 (http://frodo.wi.mit.edu/cgi-bin/primer3/primer3_www.cgi) and the human ABCA1 and β-actin sequences from the National Center for Biotechnology Information database. Sense and antisense primers were as follows: for ABCA1, 5′-CTGCTAAGGAGGGAGCCTTT-3′ and 5′-AAAAGGGCCACAAACTGTTG-3′; and for β-actin, 5′-CTATCCCTGTACGCCTCTGGC-3′ and 5′-GGCGTACAGGTCTTTGCGGATG-3′, respectively. Ethidium bromide-stained gels were scanned using a Typhoon 8600 (Amersham). The β-actin message served as an internal control.

In vivo studies

Eight week old hTTR×TTR KO and TTR KO mice were fed for 18 weeks either a high-fat/high-cholesterol diet (regular chow supplemented with 0.2% cholesterol and 21% fat; Mucedola) or a control diet (regular chow; Mucedola). After this period, sHDL particles were isolated from plasma by precipitation (Randox) and HDL-cholesterol levels were determined using an enzymatic colorimetric assay (Randox), according to the manufacturer's instructions.

LCAT activation assay

The LCAT assay was carried out using as substrate rHDL particles (incubated overnight at 37°C in the presence or absence of an equimolar amount of TTR) and 75 μl of lipoprotein-deficient serum (1.8 μg/μl total protein, fraction with d > 1.21 obtained after ultracentrifugation to isolate sHDL particles) as the enzyme source. Reaction mixes were further supplemented with 4% FAF-BSA and 4 mM β-mercaptoethanol and incubated for 1 h at 37°C. Parallel reactions performed by omitting lipoprotein-deficient serum from the reaction mix served as negative controls. Lipids were subsequently extracted twice with a 1:2 chloroform-methanol solution. The extracts were collected, dried under a nitrogen stream, and dissolved in 10 μl of the 1:2 chloroform-methanol solution. Samples were applied to thin-layer chromatography plates (Merck) using chloroform-methanol-ammonium (95:5:0.8, v/v/v) as running solvent. Free and esterified cholesterol were quantified by densitometry, and LCAT activity was measured as the ratio between esterified cholesterol and total cholesterol (free + esterified).

Binding assays to the hepatic receptor SR-BI

sHDLs were iodinated according to the iodogen method (3). Briefly, 15 μg of sHDL was added to reaction tubes coated with 10 μg of iodogen (Sigma) and containing 100 μl of 0.25 M phosphate buffer and 1 mCi of Na-^{125}I (Perkin-Elmer). The reaction was allowed to proceed in an ice bath for 20 min. Labeled sHDL was separated from free iodide in a 5 ml Sephadex G50 column (GE Healthcare). Low density lipoprotein receptor-deficient Chinese hamster ovary cells overexpressing SR-BI (IdlA7-mSRBI) and untransfected cells (IdlA7) were a kind gift from Dr. Monty Krieger (Massachusetts Institute of Technology, Cambridge). Cells were grown to confluence on 24-well plates (Corning) in Ham's F12 medium (Invitrogen) containing 5% fetal bovine serum, 2 mM glutamine (Invitrogen), 50 U/ml penicillin, 50 μg/ml streptomycin, and 500 μg/ml G418 (Calbiochem; complete medium). For competition assays, cells were washed in PBS and refed with 0.3 ml of Ham's F12 medium containing 0.5% FAF-BSA and ^{125}I-labeled sHDL (100,000 cpm/well) in the presence of unlabeled competitors. As unlabeled competitors, sHDLs (either untreated or previously treated with recombinant TTR, as described above) were used at concentrations ranging from 0 to 100 μg/ml. After 4 h of incubation at 4°C, cells were washed twice with ice-cold PBS and lysed with 1 M NaOH, after which cell-associated radioactivity was measured. Results were analyzed using GraphPad Prism software (Prism).

Circular dichroism spectroscopy

A stock solution of intact apoA-I was prepared at 0.16 mg/ml in 5 mM Tris, pH 7, for spectroscopy and biophysical analysis. TTR-cleaved apoA-I (apoA-IΔ226-243) was obtained by incubation of apoA-I with TTR at 37°C during 60 h. This extended incubation time was used to obtain 100% of the cleaved apoA-I product. For TTR removal, the reaction mixtures were passed through a Hi-Trap column (Amersham) coupled to a polyclonal anti-human TTR antibody (DAKO). The absence of TTR was confirmed by running the preparation on SDS-PAGE gels. After TTR removal, the apoA-IΔ226-243 sample was prepared at a concentration of 0.16 mg/ml in 5 mM Tris, pH 7. Protein concentrations were determined by the Bradford method (Bio-Rad). Circular dichroism (CD) spectra were recorded in a Jasco J-815 spectropolarimeter equipped with Peltier temperature control and cell stirring. Far-ultraviolet (UV) CD spectra were recorded using 1 mm pathlength polarimetrically certified cells (Hellma). Unless stated otherwise, spectra were the result of 10 averaged spectra measured at 20°C, from 190 to 260 nm, at 0.2 nm data pitch, with a 2 nm bandwidth at 100 nm/min. The program CDNN (Gerald Böhm, Martin-Luther-Universität, Halle-Witthenberg, Germany), a neural network circular dichroism deconvolution program trained from a built-in database com-

prising 33 reference spectra, was used for the analysis of secondary structure.

Dynamic light scattering

Dynamic light scattering measurements were carried out in a Malvern Zetasizer nano ZS instrument equipped with a 4 MW He-Ne Laser (632 nm). Intact apoA-I and apoA-IΔ226-243 (0.16 mg/ml in 5 mM Tris, pH 7) were centrifuged before measurements, and a 1 × 1 cm quartz cuvette (Hellma) was used. The operating procedure was typically set to 20 runs, each being averaged for 20 s. Data were analyzed using DTS software (Malvern) with respect to the distribution of particle diameter by volume.

Fluorescence spectroscopy

Fluorescence spectroscopy measurements were carried out in a Varian-Eclipse fluorimeter with Peltier temperature control at protein concentrations of 2.1 μM (intact apoA-I) and 2.3 μM (apoA-IΔ226-243). Excitation was set to 295 nm, and emission spectra were recorded between 300 and 500 nm. Excitation and emission slits were set to 10 nm.

ApoA-I fibrillogenesis studies

For apoA-I fibril formation analysis, 200 μg of apoA-I was incubated with or without an equimolar amount of TTR in 50 mM Tris, pH 7, overnight at 37°C. TTR removal from the cleavage reaction was performed as described for the CD studies. The flow-through fractions (containing only apoA-I) were dialyzed in water, pH 7, using dialysis tubing with a cutoff of 7 kDa (allowing removal of the low molecular weight apoA-I fragments), concentrated, resuspended at 2 mg/ml in 100 μl of 100 mM Tris, pH 7.4, containing 0.2% azide, and incubated for 10 days at room temperature. As a negative control, TTR alone (the same amount as that used to cleave apoA-I) was passed through the Hi-Trap column and the flow-through was used for further analysis. For electron microcopy, 5 μl aliquots of each reaction (apoA-I alone, apoA-I plus TTR, or TTR alone) were applied onto glow-discharged carbon-coated collodion films supported on 200 mesh copper grids. For negative staining, the grids were washed with deionized water and stained with 1% uranyl acetate. The grids were visualized with a Zeiss 902A microscope operated at 50 kV and examined exhaustively.

RESULTS

TTR cleaves preferentially lipid-free and poorly lipidated apoA-I

We previously determined that TTR is able to cleave the C terminus of lipid-free apoA-I after phenylalanine 225 (5). To further analyze the putative physiological consequences of this cleavage, we evaluated the ability of TTR to cleave apoA-I present in different HDL particles, namely in rHDL and sHDL isolated from human plasma (mainly composed of α-HDL but also containing a minor subpopulation of preβ-HDL particles). We observed that TTR cleaves not only lipid-free apoA-I, as determined previously, but also lipidated apoA-I; SDS-PAGE analysis showed the appearance of an ~26 kDa band after treatment of either lipid-free apoA-I or apoA-I present in rHDL particles (**Fig. 1A**, left and middle panels, respectively). The extent of lipid-free apoA-I cleavage by TTR was 37 ± 4%, whereas the extent of rHDL apoA-I cleavage was only 10 ± 1%. In the case of sHDL, although the appearance of an apoA-I fragment was not observed upon TTR treatment, a reduction of ~7 ± 1% in the intensity of intact apoA-I was seen (Fig. 1A, right panel). Regarding the extent of rHDL and sHDL cleavage by TTR, similar results were obtained by performing quantification on Coomassie Blue-stained SDS-PAGE gels or on Western blots (data not shown). These data show that apoA-I cleavage by TTR was more effective in lipid-free apoA-I and lipid-poor rHDL (which mimic nascent discoidal preβ-HDL particles) than in the fully lipidated sHDL particles. To further substantiate this observation, we analyzed by agarose electrophoresis the ability of TTR to cleave the α and preβ subpopulations present in sHDL. After treatment with TTR, a preferential loss of the preβ-HDL subpopulation was observed (Fig. 1B): a 40 ± 9% decrease of preβ-HDL particles was detected, whereas a decrease of only 13 ± 3% of α-HDL was seen (Fig. 1B), further supporting the notion that apoA-I present in lipid-rich particles is more resistant to TTR-mediated proteolysis.

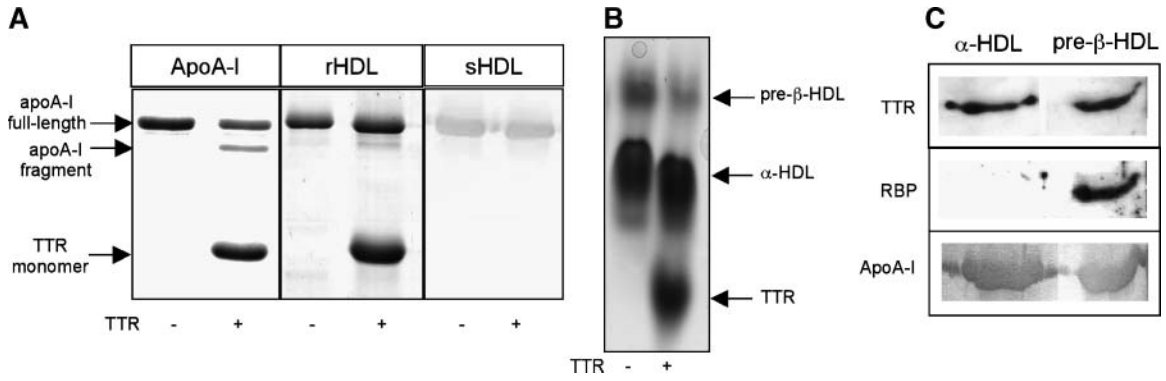

Fig. 1. Transthyretin (TTR)-mediated proteolysis of lipid-free apolipoprotein A-I (apoA-I), reconstituted discoidal preβ-migrating high density lipoprotein (rHDL), and spherical high density lipoprotein (sHDL). A: Left and middle panels, SDS-PAGE analysis of lipid-free apoA-I and rHDL incubated with (+) or without (−) recombinant TTR. Right panel, anti-apoA-I Western analysis of sHDL incubated with (+) or without (−) recombinant TTR. B: Agarose electrophoresis of human sHDL incubated either with (+) or without (−) TTR. C: Western analysis for TTR, retinol binding protein (RBP), and apoA-I present in α-HDL and preβ-HDL subpopulations from human sHDL.

In addition to the predominant lipid-free form of TTR found in the plasma, a small fraction (1–2%) of this protein was reported to be transported in HDL through binding to apoA-I (3). In this respect, we investigated by Western analysis in which sHDL subpopulation TTR was present. We determined that TTR was present in a similar percentage, relative to the amount of apoA-I, in both sHDL subpopulations (Fig. 1C). As the proteolytic activity of TTR is inhibited when the protein is in a complex with its ligand RBP (5), we analyzed the presence of RBP in the two subpopulations of sHDL and observed that RBP is present only in the preβ subpopulation (Fig. 1C). This suggests that the TTR fraction present in the preβ subpopulation might have its proteolytic activity inhibited by RBP.

Upon TTR cleavage, apoA-I has a decreased ability to promote cholesterol efflux

The C-terminal domain of apoA-I, including the region cleaved by TTR, is important for promoting cholesterol efflux from macrophages, where ABCA1 expression is increased upon cholesterol loading (8). To assess whether apoA-I cleaved by TTR displays functional changes affecting its ability to promote high-affinity cholesterol efflux, we compared cholesterol efflux from cholesterol-loaded THP-1 macrophages elicited by intact rHDL or rHDL previously cleaved by TTR. rHDLs were added to cholesterol-loaded THP-1 macrophages in the low range of acceptor protein concentration (25 μg/ml), in which the high-affinity efflux of cholesterol, mediated by ABCA1, has been shown to dominate (11). We observed that upon cleavage by TTR, rHDL displayed an ∼50% decreased ability to promote cholesterol efflux (**Fig. 2A**), thus showing that apoA-I function in promoting cholesterol efflux is impaired after TTR-mediated proteolysis.

To assess whether transgenic mice carrying human TTR in a TTR KO background (hTTR×TTR KO) could be used as tools to further investigate the impact of apoA-I cleavage by TTR in cholesterol efflux, we assessed the ability of human TTR to cleave mouse apoA-I. For that, sHDLs from TTR KO mice were isolated and exposed to recombinant human TTR, as detailed for human sHDL. In fact, human TTR was able to cleave not only human but also mouse apoA-I, as determined by the decrease in the intensity of mouse full-length apoA-I, upon TTR incubation (Fig. 2B). As such, the comparison of the biological properties of sHDL isolated from TTR KO and hTTR×TTR KO mice may be useful to further assess the biological consequences of apoA-I cleavage by TTR. Similar to what has been reported previously for human HDL (3), human TTR was detected in sHDL isolated by ultracentrifugation from hTTR×TTR KO mice (8 ng TTR/μg total protein). Moreover, as described above for human sHDL, sHDL from hTTR×TTR KO mice displayed TTR in both the α-HDL and preβ-HDL subpopulations (Fig. 2C). As predicted, given the presence of human TTR, sHDL from hTTR×TTR KO mice displayed an ∼50% decreased ability to induce cholesterol efflux, compared with sHDL isolated from TTR KO mice (Fig. 2D).

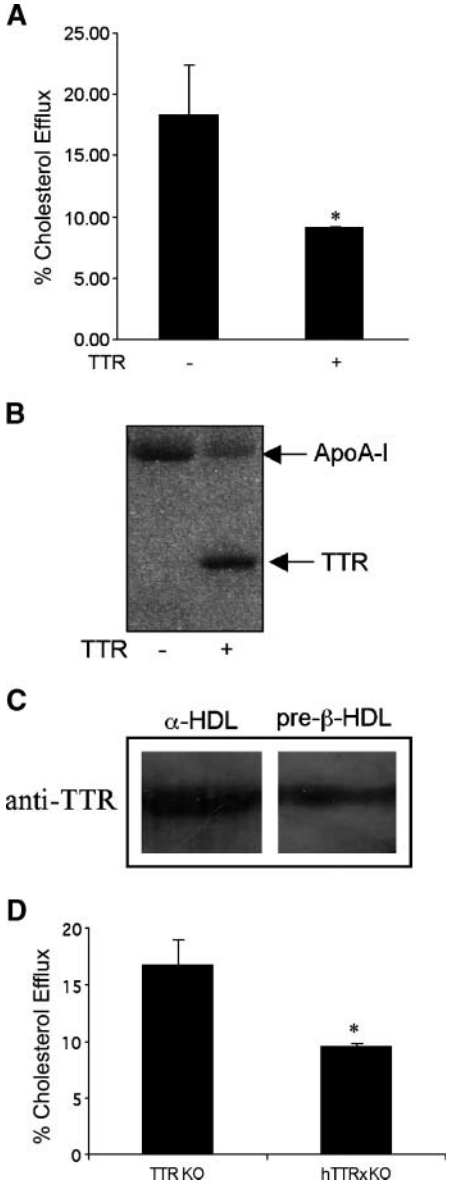

Fig. 2. ApoA-I cleaved by TTR has a decreased ability to induce cholesterol efflux. A: Percentage of cholesterol efflux from cholesterol-loaded THP-1 macrophages using as acceptor either intact rHDL (−) or rHDL cleaved by TTR (+). B: SDS-PAGE analysis of sHDL isolated from TTR KO mice incubated in the absence (−) or in the presence (+) of recombinant human TTR. C: TTR Western analysis of α-HDL and preβ-HDL subpopulations from hTTR× TTR KO mouse sHDL. D: Percentage of cholesterol efflux from cholesterol-loaded THP-1 macrophages using as cholesterol acceptors sHDL isolated from TTR KO mouse plasma or hTTR× TTR KO mouse plasma. Error bars indicate ± SD. * $P < 0.05$.

This result led us to measure HDL-cholesterol in both strains when fed a high-fat/high-cholesterol diet. TTR KO mice fed a high-fat/high-cholesterol diet had a 2.1-fold increase in the amount of cholesterol transported in HDL compared with the same mouse strain fed with regular chow, whereas in hTTR×TTR KO mice this increase was only 1.3-fold. This result further supports the hypothesis that TTR diminishes the ability of HDL to perform reverse cholesterol transport.

ApoA-I cleaved by TTR has decreased ability to bind to ABCA1

The diminished capacity of apoA-I cleaved by TTR to induce cholesterol efflux from THP-1 cells suggested that C-terminally deleted apoA-I has a decreased capacity to bind ABCA1, as described previously (23). To further address this issue, we performed cholesterol efflux assays in HEK293 cells untransfected or transfected with ABCA1 (24), using as cholesterol acceptor apoA-I (either intact or cleaved by TTR). The expression of ABCA1 in HEK293-ABCA1 cells and its absence in HEK293 untransfected cells was confirmed by RT-PCR (**Fig. 3A**). In untransfected HEK293 cells, the values of cholesterol efflux were residual and unaffected by TTR (Fig. 3B). As predicted given the expression of the receptor, HEK293-ABCA1 cells presented an increase in the rate of cholesterol efflux compared with untransfected cells. Moreover, in HEK293-ABCA1 cells, cleavage of apoA-I by treatment with TTR led to an ~50% decrease in the rate of cholesterol efflux (Fig. 3B), suggesting that the apoA-I fragment generated by TTR proteolysis has a reduced ability to bind to ABCA1.

ApoA-I cleavage by TTR has no effect on LCAT activation

To evaluate whether the proteolytic modification of apoA-I by TTR also alters its ability to activate LCAT, we compared the esterification of cholesterol induced by intact rHDL with that induced by TTR-cleaved rHDL. No changes in the rates of cholesterol esterification were observed after proteolysis of rHDL by TTR (data not shown), suggesting that apoA-I degradation by TTR does not decrease its capacity to activate LCAT.

TTR cleavage of apoA-I present in sHDL does not affect binding to SR-BI

Besides cholesterol efflux, another crucial step in reverse cholesterol transport is the SR-BI-mediated selective uptake of CE in the liver that occurs upon the interaction of SR-BI with apoA-I present in α-HDL. In this respect, we investigated the impact of apoA-I cleavage by TTR in the SR-BI binding of intact sHDL and sHDL cleaved by TTR. This study was performed through competition assays using a cell line overexpressing murine SR-BI (IdlA7-mSRBI). Both intact sHDL and sHDL cleaved by TTR competed similarly with ^{125}I-sHDL binding to the receptor (**Fig. 4**). As a control, the assay was performed using TTR as a competitor; in this case, no binding to SR-BI was observed (data not shown), as described previously (25), showing that TTR itself does not interfere in the assay. Moreover, assays performed with untransfected IdlA7 cells showed no binding of sHDL (data not shown). In conclusion, under physiological conditions, TTR probably does not affect sHDL recognition by SR-BI as a consequence of the minute cleavage of apoA-I by TTR when apoA-I is present in fully lipidated particles.

In vitro, TTR increases apoA-I aggregation and fibril formation

Amyloid deposits in the aortic intima are very common in association with atherosclerosis: N-terminal fragments of apoA-I deposited as amyloid fibrils are present in human atherosclerotic plaques (16). Proteolysis has been thought to play an important role in most types of amyloidoses; in several cases, an amyloid peptide is generated by proteolytic cleavage of the corresponding protein precursor. We hypothesized that cleavage of the C terminus of apoA-I by TTR might influence its deposition as amyloid. To evaluate this hypothesis, the structural consequences of apoA-I cleavage by TTR, as well the amyloidogenicity of full-length apoA-I and of TTR-cleaved apoA-I, were compared using several biophysical methodologies. We started by analyzing the structural consequences of apoA-I cleavage by TTR, by comparing the relative content of α-helices by far-UV CD of intact apoA-I and apoA-IΔ226-243 (**Table 1**). The percentage of α-helices (45%) of freshly prepared intact apoA-I (as prepared) compared very well with the value reported in the literature [44% (26)]. On the other hand, intact apoA-I prepared under the conditions in which the proteolytic digestion was carried out (proteolysis conditions) had a substantially lower α-helix content that was identical to the one obtained for

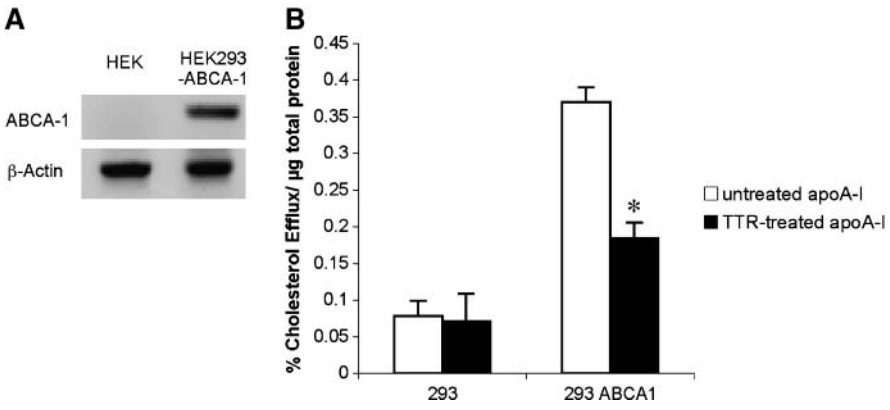

Fig. 3. ApoA-I cleaved by TTR has reduced ability to bind to ABCA1. A: RT-PCR analysis of ABCA1 expression in HEK293 cells either untransfected (HEK293) or transfected with ABCA1 (HEK293-ABCA1). B: Rate of cholesterol efflux from HEK293 cells untransfected or transfected with ABCA1 using as cholesterol acceptors either lipid-free untreated apoA-I or TTR-treated apoA-I. Error bars indicate ± SD. * $P < 0.05$.

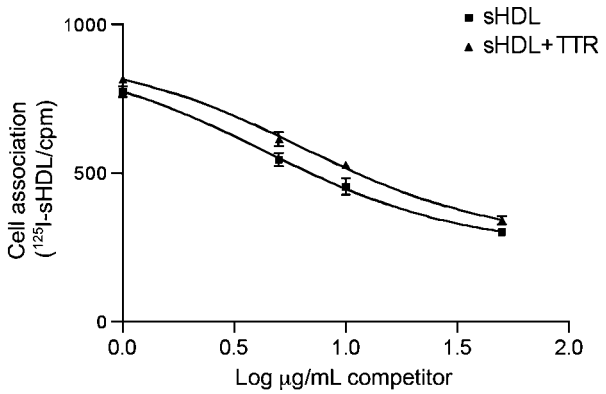

Fig. 4. Cleavage of apoA-I present in sHDL by TTR does not affect binding to scavenger receptor class B type I. Cell association of ^{125}I-sHDL to IdlA7-mSRBI cells is shown. Competition was by either intact sHDL (sHDL) or sHDL previously treated with TTR (sHDL + TTR) at increasing concentrations ranging from 0 to 100 μg/ml. Error bars indicate ± SD.

apoA-IΔ226-243 (Table 1). From the analysis of the secondary structure content, it seems that the loss in α-helices resulted mostly in β-strand formation and an increase in random conformations for both intact apoA-I and apoA-IΔ226-243. In conclusion, under the studied conditions, there was no significant difference in the α-helical content of apoA-I (under proteolysis conditions) and its cleaved form apoA-IΔ226-243, in accordance with previous reports (27).

Considering the relatively long incubation period required to achieve the highest yield possible of apoA-IΔ226-243, the possibility that apoA-I aggregates or oligomers were being formed was investigated by dynamic light scattering (**Fig. 5A**). The data obtained demonstrated that, in the absence of TTR, apoA-I was not aggregating during the 60 h of incubation at 37°C (particle size variation from 5.4 to 5.5 nm). On the other hand, large particles corresponding to aggregates were observed for apoA-IΔ226-243 (from 38 to 154 nm particles). These results suggest that by cleaving the 226–243 apoA-I C-terminal region, TTR increases the aggregation propensity of apoA-I. Moreover, dynamic light scattering analysis of apoA-I after thermal unfolding showed that, whereas the size of intact apoA-I particles changed very modestly (from 5.2 to 7.2 nm) in apoA-IΔ226-243, even larger particles were observed than before thermal denaturation (~90 and 300 nm), suggesting that thermal perturbation further enhances aggregation propensity in this variant (data not shown).

To monitor differences in the tertiary structure contacts of intact apoA-I (freshly prepared and prepared under proteolysis conditions) and apoA-IΔ226-243, we assessed tryptophan fluorescence emission. The position of the emission maximum obtained upon selective excitation of the tryptophan moieties at 295 nm provides an indication of the environment around this residue: increasing exposure to solvent water red-shifts the emission maximum up to 355 nm, which corresponds to a fully solvent-exposed residue. ApoA-I contains four tryptophan residues, none in the cleaved region. ApoA-I incubation at 37°C during 60 h, compared with nonincubated intact apoA-I, results in a decrease of tryptophan emission intensity and a slight red shift to 346 nm (Fig. 5B), suggesting a conformational change. This observation agrees well with the loss of secondary structure seen by far-UV CD and with the slight particle size increase observed by dynamic light scattering. ApoA-IΔ226-243 is clearly more conformationally altered, considering the red shift of the emission maximum at 20°C and the lowest fluorescence intensity (Fig. 5B). We further analyzed the thermal unfolding of intact apoA-I (freshly prepared and prepared under proteolysis conditions) and apoA-IΔ226-243 by tryptophan fluorescence emission and verified that, whereas the thermal unfolding of intact apoA-I is fully reversible, that of apoA-IΔ226-243 was only partially reversible (Fig. 5B). This behavior agrees well with a less organized fold of the apoA-IΔ226-243 variant, compatible with the presence of aggregates and/or overall conformational destabilization resulting from the cleavage.

To further verify the hypothesis that apoA-I cleaved by TTR might be aggregating and forming fibrils, analysis of fibrillar growth by transmission electron microcopy was performed. We observed that after 10 days of incubation under conditions promoting fibrillar growth (28), cleaved apoA-I already presented fibrils, in contrast to the full-length protein, in which fibril formation was still not observed (Fig. 5C), thereby supporting the notion that cleavage of apoA-I by TTR enhances apoA-I deposition in the form of amyloid fibrils. In the control preparation starting with TTR alone, no fibrils were observed in the grid (data not shown), clearly demonstrating that fibrils observed when apoA-I is cleaved by TTR are not the result of a putative TTR contamination in the preparation.

TABLE 1. Secondary structure content in apoA-I forms determined by far-ultraviolet circular dichroism

	Secondary Structure Content		
Protein	α-Helix	β-Strands	Random Coil
		%	
ApoA-I[a]	45 ± 2	29	27
ApoA-I[b]	14 ± 1	51	35
ApoA-IΔ226-243	16 ± 1	48	34

ApoA-I, apolipoprotein A-I.
[a] As prepared.
[b] Under proteolysis conditions (60 h at 37°C).

DISCUSSION

Previous in vitro studies demonstrated that several proteases, including matrix metalloproteases (14), plasmin and kallikrein (15), and two mast cell proteases, chymase and tryptase (8), can degrade apoA-I present in preβ-HDL particles, thereby impairing cellular cholesterol efflux. In this report, we show that TTR has a similar effect: not only does TTR cleave apoA-I in the C terminus after the same residue as chymase (phenylalanine 225) (5), but TTR also is more effective at cleaving apoA-I present in lipid-poor

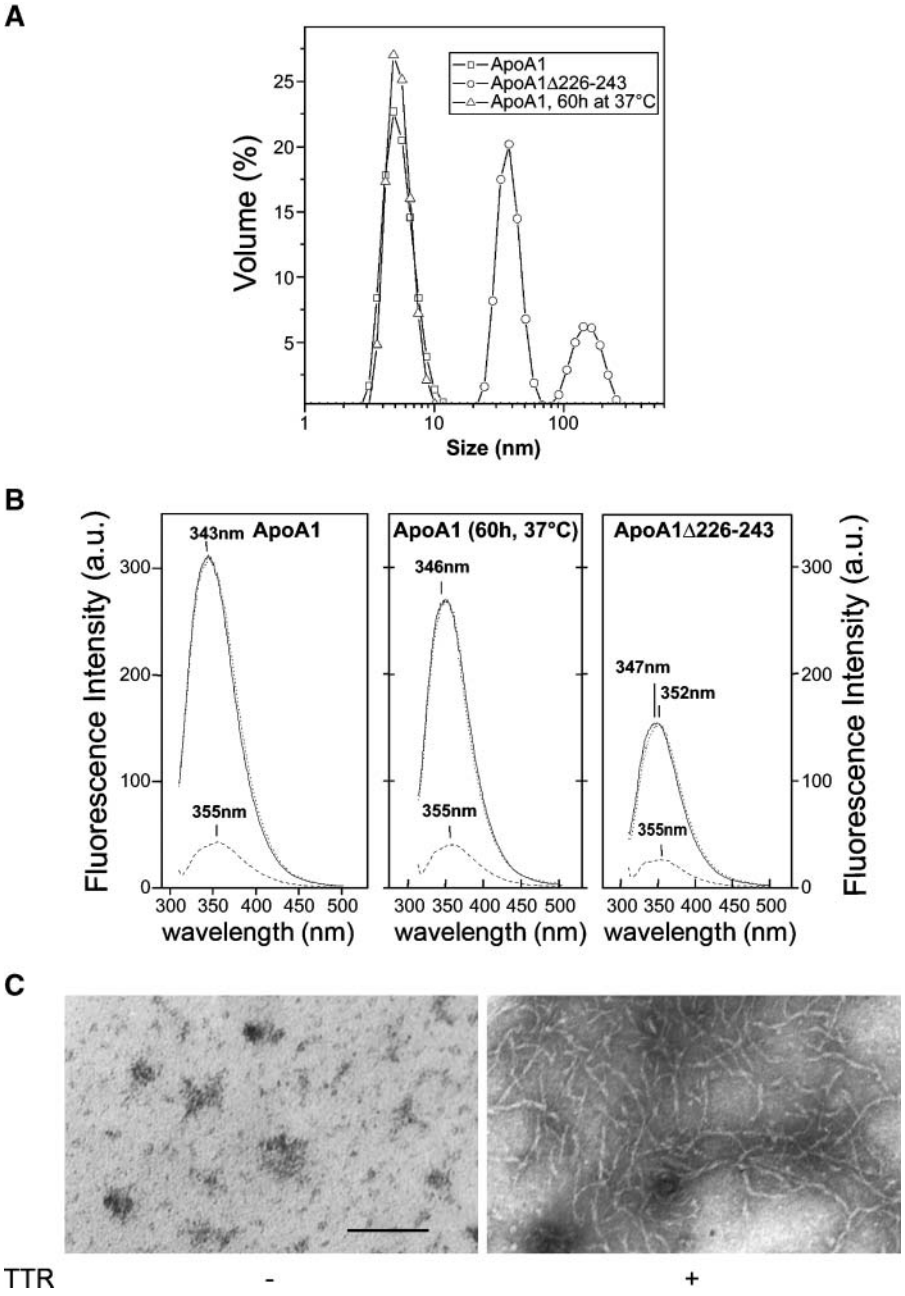

Fig. 5. In vitro, TTR increases apoA-I aggregation and fibril formation. A: Particle size distribution by volume (nm/%) determined from dynamic light-scattering measurements on freshly prepared apoA-I (squares; 5.42 nm/99.8%), apoA-I incubated for 60 h at 37°C (triangles; 5.47 nm/99.8%), and apoA-IΔ226-243 (circles; 38.4nm/70.9% and 154.5 nm/29.1%). B: Fluorescence tryptophan emission spectra of intact apoA-I (left panel), intact apoA-I incubated for 60 h at 37°C (middle panel), and apoA-IΔ226-243 (right panel) recorded at 20°C (solid lines), at 95°C (dashed lines), and after cooling back to 20°C (dotted lines). a.u., arbitrary units. C: Electron microscopy of negatively stained apoA-I fibrils (bar = 100 nm) previously incubated in the absence (−) or presence (+) of TTR.

preβ-HDL particles, resulting in an impairment in the ability of rHDL to promote cholesterol efflux from macrophages. The reason underlying the increased susceptibility for proteolysis of apoA-I in lipid-poor preβ-HDL is probably related to an increased exposure of domains vulnerable to protease attack compared with apoA-I in large spherical α-HDL (12). Despite a low extent of proteolysis, rHDLs have an ~50% decreased ability to promote cholesterol efflux. The same was observed with plasmin and kallikrein, two plasma proteases found in the arterial intima, which only produce a slight loss of apoA-I in HDL_3 (ultracentrifugally separated particles with d = 1.125–1.21, containing preβ-HDL) but lead to an ~50% decrease in HDL_3-mediated cholesterol efflux (15). Although, as documented above, a number of proteases cleave rHDL particles to a small extent, this cleavage results in a

considerable decrease in the ability of the particle to perform cholesterol efflux; the reason underlying this apparent discrepancy is unclear.

Under physiological conditions, it was previously determined that 1–2% of human plasma TTR circulates in HDL through binding to apoA-I (3), but the relevance of this finding remained obscure. In that study, TTR was not detected in HDL from hTTR×TTR KO mice, probably because gel filtration instead of ultracentrifugation was used as the method of HDL isolation. We now show that, as in humans, TTR is present in sHDL isolated from transgenic mice for human TTR. Moreover, these particles have a decreased ability to promote cholesterol efflux compared with sHDL particles isolated from TTR KO mice, further suggesting that TTR, either present in HDL or circulating in the plasma, may affect HDL biology. Also, we found that when fed a high-fat/high-cholesterol diet, hTTR×TTR KO mice present a lower HDL-cholesterol increase compared with TTR KO mice. This observation probably results from a decreased ability of HDL from hTTR×TTR KO mice to mediate cholesterol efflux, as a consequence of apoA-I cleavage by TTR. In our studies, we were unable to observe apoA-I fragments in the sHDL particles isolated from either hTTR×TTR KO mice or human plasma samples, which would further confirm apoA-I proteolysis by TTR in vivo. This might be related to a low cleavage of sHDL particles by TTR. In this respect, it is interesting that upon cleavage, N-terminal apoA-I fragments have been shown to dissociate from lipids (29), precluding the isolation at d = 1.063–1.210 g/ml of preβ particles containing C-terminally deleted apoA-I. This most likely results from the fact that the C-terminal portion of apoA-I determines intimate contact with lipids. Moreover, the fact that truncated forms of apoA-I lacking the C terminus cannot associate with HDL might explain the fast catabolism of N-terminal proteolytic apoA-I fragments.

ApoA-I is responsible for the major functions of HDL: its central region has been implicated in the activation of LCAT (7), whereas its C-terminal domain is crucial for the induction of cholesterol efflux (4). Concerning the mechanism of cholesterol efflux, it may occur through two distinct mechanisms: *i*) lipid-free or lipid-poor apolipoproteins promote the efflux of free cholesterol by interacting with ABCA1 in the cell membrane; and *ii*) mature HDL can acquire free cholesterol by aqueous diffusion mediated by SR-BI. In this work, using THP-1 cells, we show that TTR proteolysis of rHDL decreases the ABCA1-mediated component of cholesterol efflux, as our experiments were performed in the low range of acceptor protein concentration, at which the cholesterol efflux mediated by this receptor dominates. This was further confirmed in cholesterol efflux assays using HEK293 cells either untransfected or transfected with ABCA1; in that assay, cleavage of apoA-I by TTR decreased the rate of cholesterol efflux by HEK293-ABCA1 cells, further supporting the notion that the effect of TTR on apoA-I-mediated cholesterol efflux is ABCA1-dependent. Moreover, this result suggests that apoA-I cleaved by TTR has reduced affinity for ABCA1, as it has been shown that the ability of apoA-I to bind ABCA1, as assessed by cross-linking, is correlated with the ability of the protein to induce cholesterol efflux (30). In that report, C-terminal mutants of apoA-I lacking the 220–231 region presented a decreased ability to bind ABCA1 and to promote lipid efflux (30). Our results are in agreement with that study, as the apoA-I fragment generated by TTR proteolysis lacks part of the crucial region mediating the interaction with ABCA1 and, as such, cholesterol efflux is affected.

In relation to LCAT, rHDL cleavage by TTR did not alter its ability to activate this enzyme. This result is in accordance with the fact that the central region of apoA-I, and not the C-terminal domain of the protein, is thought to be important for LCAT activation (7). Interestingly, similar limited proteolysis of apoA-I in rHDL by four different proteases (chymotrypsin, trypsin, elastase, and subtilisin) has been reported to produce a relatively stable N-terminal polypeptide of ~22 kDa, which retains LCAT activation (13).

Another important step in the mechanism of reverse cholesterol transport is the selective uptake of HDL-CE mediated by SR-BI that occurs in the liver and steroidogenic tissues (10). Efficient functioning of SR-BI depends on the productive binding of apoA-I to the receptor. Although the precise apoA-I binding site for SR-BI has not been identified, previous reports showed that the C-terminal region of apoA-I is important for SR-BI recognition (31). However, we observed that apoA-I cleavage by TTR had no effect on sHDL binding to SR-BI, probably as a consequence of the minute cleavage of the spherical particles by TTR.

Intimal amyloid associated with atherosclerotic plaques is derived from a major N-terminal fragment (1–69) of apoA-I (16). Several amyloid fibril proteins are also composed of fragments of larger precursors, indicating that a proteolytic step is important in the pathogenesis of the amyloid forms, possibly by uncovering a normally hidden fibrillogenic fragment in the precursor. In this respect, it is possible that upon TTR cleavage, apoA-I becomes more prone to fibril formation. Under the conditions used, upon incubation of lipid-free apoA-I with TTR, a single 26 kDa apoA-I fragment is formed. To address the stability of the apoA-I fragment generated by TTR proteolysis (apoA-IΔ226-243), we performed circular dichroism experiments. Under extended incubation times similar to those used to obtain 100% cleavage, intact apoA-I had an identical α-helix content to the one obtained for apoA-IΔ226-243. This is in accordance with previous experiments that have shown that in lipid-free conditions, there is little difference in the α-helical content of apoA-I (44 ± 3%) and apoA-IΔ223-243 (40 ± 2%); apoA-I Δ223-243 is the reported C-terminal apoA-I deletion closest to the one performed by TTR (27). That difference became significant only in the presence of lipids (69% for intact apoA-I vs. 45% for the cleaved form of the protein). However, we observed that apoA-IΔ226-243 presents an overall conformational destabilization and a higher propensity for aggregation compared with intact apoA-I. Moreover, in conditions promoting fibril formation, apoA-IΔ226-243 formed fibrils but the intact protein did not. The hypothesis that TTR might intervene in

apoA-I fibril formation had been raised previously. Under pathological conditions, amyloid fibrils from a patient carrying an apoA-I mutation presented both apoA-I N-terminal fragments and wild-type TTR (6), suggesting that TTR might influence the generation of apoA-I fragments and apoA-I deposition. In summary, we have now shown that apoA-I cleaved by TTR has a higher propensity to form aggregates than intact apoA-I and forms fibrils faster than the full-length protein, suggesting that TTR increases apoA-I amyloidogenicity in vitro.

This work shows that the TTR-apoA-I interaction is important under both physiological and pathological conditions. TTR may intervene in HDL biology and in atherosclerosis by reducing HDL-mediated cholesterol efflux and by increasing apoA-I amyloidogenicity. The question arising from our results is this: is TTR present in a proteolytic active form in the microenvironment surrounding foam cells? Most TTR circulates in the plasma in the lipid-free form, but 1–2% of the protein circulates in HDL in both the preβ and α subpopulations. There is no evidence for the presence of plasmatic TTR in the intima; however, the extracellular fluid of the intima is rich in lipid-poor HDL species, such as preβ-HDL, that promote cholesterol efflux from macrophages. This issue raises a second question: is the TTR fraction present in preβ-HDL active, and by degrading apoA-I does it act as a local modulator of cholesterol efflux from foam cells? Moreover, RBP (a TTR ligand that inhibits its proteolytic activity) could only be detected in the preβ subpopulation. It is noteworthy that our previous studies (3) did not detect RBP in HDL isolated by gel filtration, probably as a consequence of the different isolation method of the particles. Although we now show that both TTR and RBP are present in preβ-HDL, we cannot be sure that in this subpopulation TTR is complexed with RBP, as it may be bound to other lipoprotein components. Even if in preβ-HDL, TTR and RBP are present as a complex, circulating preβ-HDL could still be degraded by lipid-free TTR, which is the major form of the protein present in the plasma. In any of these scenarios, TTR might cleave the C terminus of apoA-I, reducing its capacity to promote HDL-mediated cholesterol efflux and increasing apoA-I amyloidogenicity.

The authors thank Rui Fernandes (Advanced Tissue Analysis Facility, Instituto de Biologia Molecular e Celular, Porto, Portugal) for assistance in electron microscopy studies. This project was supported by grants from the Fundação Calouste Gulbenkian, Portugal, and the Association Française Contre les Myopathies, France. M.A.L. is the recipient of a fellowship (SFRH/BD/17253/2004) from the Fundação para a Ciência e Tecnologia, Portugal.

REFERENCES

1. Blake, C. C., M. J. Geisow, S. J. Oatley, B. Rerat, and C. Rerat. 1978. Structure of prealbumin: secondary, tertiary and quaternary interactions determined by Fourier refinement at 1.8 A. *J. Mol. Biol.* **121:** 339–356.
2. Monaco, H. L. 2000. The transthyretin-retinol-binding protein complex. *Biochim. Biophys. Acta.* **1482:** 65–72.
3. Sousa, M. M., L. Berglund, and M. J. Saraiva. 2000. Transthyretin in high density lipoproteins: association with apolipoprotein A-I. *J. Lipid Res.* **41:** 58–65.
4. Lee, M., P. T. Kovanen, G. Tedeschi, E. Oungre, G. Franceschini, and L. Calabresi. 2003. Apolipoprotein composition and particle size affect HDL degradation by chymase: effect on cellular cholesterol efflux. *J. Lipid Res.* **44:** 539–546.
5. Liz, M. A., C. J. Faro, M. J. Saraiva, and M. M. Sousa. 2004. Transthyretin, a new cryptic protease. *J. Biol. Chem.* **279:** 21431–21438.
6. de Sousa, M. M., C. Vital, D. Ostler, R. Fernandes, J. Pouget-Abadie, D. Carles, and M. J. Saraiva. 2000. Apolipoprotein AI and transthyretin as components of amyloid fibrils in a kindred with apoAI Leu178His amyloidosis. *Am. J. Pathol.* **156:** 1911–1917.
7. Uboldi, P., M. Spoladore, S. Fantappie, S. Marcovina, and A. L. Catapano. 1996. Localization of apolipoprotein A-I epitopes involved in the activation of lecithin:cholesterol acyltransferase. *J. Lipid Res.* **37:** 2557–2568.
8. Lee-Rueckert, M., and P. T. Kovanen. 2006. Mast cell proteases: physiological tools to study functional significance of high density lipoproteins in the initiation of reverse cholesterol transport. *Atherosclerosis.* **189:** 8–18.
9. Lee, M., C. P. Sommerhoff, A. von Eckardstein, F. Zettl, H. Fritz, and P. T. Kovanen. 2002. Mast cell tryptase degrades HDL and blocks its function as an acceptor of cellular cholesterol. *Arterioscler. Thromb. Vasc. Biol.* **22:** 2086–2091.
10. Landschulz, K. T., R. K. Pathak, A. Rigotti, M. Krieger, and H. H. Hobbs. 1996. Regulation of scavenger receptor, class B, type I, a high density lipoprotein receptor, in liver and steroidogenic tissues of the rat. *J. Clin. Invest.* **98:** 984–995.
11. Favari, E., M. Lee, L. Calabresi, G. Franceschini, F. Zimetti, F. Bernini, and P. T. Kovanen. 2004. Depletion of pre-beta-high density lipoprotein by human chymase impairs ATP-binding cassette transporter A1- but not scavenger receptor class B type I-mediated lipid efflux to high density lipoprotein. *J. Biol. Chem.* **279:** 9930–9936.
12. Kunitake, S. T., G. C. Chen, S. F. Kung, J. W. Schilling, D. A. Hardman, and J. P. Kane. 1990. Pre-beta high density lipoprotein. Unique disposition of apolipoprotein A-I increases susceptibility to proteolysis. *Arteriosclerosis.* **10:** 25–30.
13. Ji, Y., and A. Jonas. 1995. Properties of an N-terminal proteolytic fragment of apolipoprotein AI in solution and in reconstituted high density lipoproteins. *J. Biol. Chem.* **270:** 11290–11297.
14. Lindstedt, L., J. Saarinen, N. Kalkkinen, H. Welgus, and P. T. Kovanen. 1999. Matrix metalloproteinases-3, -7, and -12, but not -9, reduce high density lipoprotein-induced cholesterol efflux from human macrophage foam cells by truncation of the carboxyl terminus of apolipoprotein A-I. Parallel losses of pre-beta particles and the high affinity component of efflux. *J. Biol. Chem.* **274:** 22627–22634.
15. Lindstedt, L., and P. T. Kovanen. 2000. Plasmin and kallikrein reduce HDL-induced cholesterol efflux from foam cells. *Biochem. Biophys. Res. Commun.* **277:** 552–557.
16. Westermark, P., G. Mucchiano, T. Marthin, K. H. Johnson, and K. Sletten. 1995. Apolipoprotein A1-derived amyloid in human aortic atherosclerotic plaques. *Am. J. Pathol.* **147:** 1186–1192.
17. Episkopou, V., S. Maeda, S. Nishiguchi, K. Shimada, G. A. Gaitanaris, M. E. Gottesman, and E. J. Robertson. 1993. Disruption of the transthyretin gene results in mice with depressed levels of plasma retinol and thyroid hormone. *Proc. Natl. Acad. Sci. USA.* **90:** 2375–2379.
18. Monteiro, F. A., M. M. Sousa, I. Cardoso, J. B. do Amaral, A. Guimaraes, and M. J. Saraiva. 2006. Activation of ERK1/2 MAP kinases in familial amyloidotic polyneuropathy. *J. Neurochem.* **97:** 151–161.
19. Havel, R. J., H. A. Eder, and J. H. Bragdon. 1955. The distribution and chemical composition of ultracentrifugally separated lipoproteins in human serum. *J. Clin. Invest.* **34:** 1345–1353.
20. Jonas, A., K. E. Kezdy, and J. H. Wald. 1989. Defined apolipoprotein A-I conformations in reconstituted high density lipoprotein discs. *J. Biol. Chem.* **264:** 4818–4824.
21. Lowry, O. H., N. J. Rosebrough, A. L. Farr, and R. J. Randall. 1951. Protein measurement with Folin phenol reagent. *J. Biol. Chem.* **193:** 265–275.
22. Laurel, C. B. 1965. Antigen-antibody crossed electrophoresis. *Anal. Biochem.* **10:** 358–361.
23. Chroni, A., T. Liu, I. Gorshkova, H. Y. Kan, Y. Uehara, A. Von Eckardstein, and V. I. Zannis. 2003. The central helices of apoA-I can promote ATP-binding cassette transporter A1 (ABCA1)-mediated lipid efflux. Amino acid residues 220–231 of the wild-

type apoA-I are required for lipid efflux in vitro and high density lipoprotein formation in vivo. *J. Biol. Chem.* **278:** 6719–6730.
24. Brunham, L. R., R. R. Singaraja, T. D. Pape, A. Kejariwal, P. D. Thomas, and M. R. Hayden. 2005. Accurate prediction of the functional significance of single nucleotide polymorphisms and mutations in the ABCA1 gene. *PLoS Genet.* **1:** e83.
25. Sousa, M. M., and M. J. Saraiva. 2001. Internalization of transthyretin. Evidence of a novel yet unidentified receptor-associated protein (RAP)-sensitive receptor. *J. Biol. Chem.* **276:** 14420–14425.
26. Tanaka, M., P. Dhanasekaran, D. Nguyen, S. Ohta, S. Lund-Katz, M. C. Phillips, and H. Saito. 2006. Contributions of the N- and C-terminal helical segments to the lipid-free structure and lipid interaction of apolipoprotein A-I. *Biochemistry.* **45:** 10351–10358.
27. Saito, H., P. Dhanasekaran, D. Nguyen, E. Deridder, P. Holvoet, S. Lund-Katz, and M. C. Phillips. 2004. Alpha-helix formation is required for high affinity binding of human apolipoprotein A-I to lipids. *J. Biol. Chem.* **279:** 20974–20981.
28. Wisniewski, T., A. A. Golabek, E. Kida, K. E. Wisniewski, and B. Frangione. 1995. Conformational mimicry in Alzheimer's disease. Role of apolipoproteins in amyloidogenesis. *Am. J. Pathol.* **147:** 238–244.
29. Obici, L., G. Franceschini, L. Calabresi, S. Giorgetti, M. Stoppini, G. Merlini, and V. Bellotti. 2006. Structure, function and amyloidogenic propensity of apolipoprotein A-I. *Amyloid.* **13:** 191–205.
30. Chroni, A., T. Liu, M. L. Fitzgerald, M. W. Freeman, and V. I. Zannis. 2004. Cross-linking and lipid efflux properties of apoA-I mutants suggest direct association between apoA-I helices and ABCA1. *Biochemistry.* **43:** 2126–2139.
31. Liadaki, K. N., T. Liu, S. Xu, B. Y. Ishida, P. N. Duchateaux, J. P. Krieger, J. Kane, M. Krieger, and V. I. Zannis. 2000. Binding of high density lipoprotein (HDL) and discoidal reconstituted HDL to the HDL receptor scavenger receptor class B type I. Effect of lipid association and APOA-I mutations on receptor binding. *J. Biol. Chem.* **275:** 21262–21271.